

# Searching for $\gamma$ -Ray Pulsars among *Fermi* Unassociated Sources: 2FGL J1906.5+0720

Yi XING and Zhongxiang WANG

*Shanghai Astronomical Observatory, Chinese Academy of Sciences,*

*80 Nandan Road, Shanghai 200030, China*

*yixing@shao.ac.cn*

*wangzx@shao.ac.cn*

(Received ; accepted )

## Abstract

We report the results from our analysis of the *Fermi* Large Area Telescope data of the *Fermi* unassociated source 2FGL J1906.5+0720, which is a high-ranked candidate pulsar. We first update the ephemeris for PSR J1907+0602, which is used to remove any possible contamination due to strong emission from this nearby pulsar. A small glitch  $\Delta\nu/\nu \simeq 1.5 \times 10^{-9}$  is found around MJD 55866 in the pulsar. From our analysis, 2FGL J1906.5+0720 is confirmed to have a significant low energy cutoff at  $\sim 1$  GeV in its emission ( $14\sigma$ – $18\sigma$  significance), consistent with those seen in young pulsars. We search for pulsations but no spin frequency signals are found in a frequency range of 0.5–32 Hz. No single model can fully describe the source’s overall *Fermi*  $\gamma$ -ray spectrum, and the reason for this is because of excess emission detected at energies of  $\geq 4$  GeV. The high-energy component, also seen in the Crab pulsar and several  $\gamma$ -ray binaries and probably due to a cold pulsar wind, likely originates from 2FGL J1906.5+0720 as either contamination from nearby sources or existence of an extended source is excluded. We conclude that 2FGL J1906.5+0720 is likely a pulsar based on the emission properties, and radio search for pulsations is needed in order to confirm its pulsar nature.

**Key words:** Gamma rays: stars — pulsars: general — pulsars: individual (PSR J1907+0602)

## 1. Introduction

Since the *Fermi* Gamma-ray Space Telescope was launched on June 2008, the main instrument on-board—the Large Area Telescope (LAT) has been continuously scanning the whole sky every three hours in the energy range from 20 MeV to 300 GeV, discovering and monitoring  $\gamma$ -ray sources with much improved spatial resolution and sensitivity comparing to former  $\gamma$ -ray telescopes (Atwood et al.

2009). In 2012 resulting from *Fermi*/LAT data of the first two-year survey, a catalog of 1873  $\gamma$ -ray sources was released by Nolan et al. (2012) as the *Fermi*/LAT second source catalog. Among the  $\gamma$ -ray sources, approximately 800 and 250 sources were found to be respectively associated with blazars and active galaxies of uncertain types, and more than 100 sources were associated with pulsars in our Galaxy. Sources of these three types account for the majority of the  $\gamma$ -ray sources detected by *Fermi*. In addition, 575 sources in the catalog have not been associated with any known astrophysical objects (Nolan et al. 2012). The nature of these *Fermi* unassociated sources has yet to be studied.

Because of the relative lack of sources at low Galactic latitudes in many extragalactic source catalogs and the emission contamination by the Galaxy, the Galactic distribution of the *Fermi* unassociated sources were found to concentrate towards the Galactic plane (Nolan et al. 2012). More than half of the unassociated sources are located at low latitudes with  $|b| < 10^\circ$  (Nolan et al. 2012), possibly suggesting Galactic origins for most of them. Taking under consideration the types of identified and associated Galactic  $\gamma$ -ray sources in the catalog, these low-latitude unassociated sources are most likely pulsars, pulsar wind nebulae, supernova remnants, globular clusters, or high-mass binaries. Additionally since identified and associated active galactic nuclei (AGNs) or blazars have a nearly isotropic distribution, AGN/blazar origins for these sources can not be excluded. In any case, the low-latitude *Fermi* unassociated sources are the best pulsar candidates on the basis of currently known Galactic  $\gamma$ -ray populations, as  $\sim 50\%$  of the identified or associated Galactic *Fermi* sources are pulsars (Nolan et al. 2012).

Aiming to search for new pulsars among the unassociated sources, we selected the pulsar candidates from the *Fermi* second source catalog by requiring  $|b| < 10^\circ$  and variability indices (Variability\_Index parameter in the catalog) lower than 41. The variability indices were reported to measure the variability levels of sources, and a value larger than 41.64 indicates  $< 1\%$  chance of being a steady source (Nolan et al. 2012). We further ranked the candidates by their Signif\_Curve parameters reported in the catalog, which represent the significance of the fit improvement between curved spectra and power-law spectra, as  $\gamma$ -ray pulsars typically have curved spectra with a form of exponentially cutoff power law. The first ten sources from our selection are listed in Table 1. The first source listed is 2FGL J1704.9–4618, which has the highest Signif\_Curve value of  $\sim 9.97\sigma$  but the lowest detection significance value ( $\sim 9\sigma$ ; Signif\_Avg parameters in the catalog). For a comparison, the second source in our list 2FGL J1906.5+0720 has both high Signif\_Curve ( $\sim 9.85\sigma$ ) and Signif\_Avg values ( $\sim 24\sigma$ ), and is ranked the first among candidate pulsars by Lee et al. (2012), who applied a Gaussian-mixture model for the ranking. We thus carried out detailed study of 2FGL J1906.5+0720 by analyzing *Fermi*/LAT data of the source region, and report our results in this paper.

In addition, 2FGL J1906.5+0720 is located close to a very bright  $\gamma$ -ray pulsar J1907+0602 (Signif\_Avg  $\sim 55\sigma$ ; Abdo et al. 2013). The angular distance between them is approximately 1.3 degrees (see Figure 1). The pulsar was discovered in the first  $\sim 4$  month LAT data, revealed with a spin frequency of  $\sim 9.378$  Hz and a spin-down luminosity of  $\sim 2.8 \times 10^{36}$  erg s $^{-1}$  (Abdo et al. 2009). The pulsar is radio faint, making very difficult study its timing behavior at radio frequencies (Abdo et al.

2010). In order to better study our targeted *Fermi* source by removing possible contamination from PSR J1907+0602, we performed timing analysis to the LAT data of the pulsar. From our analysis, we discovered a possible new glitch in the data of the pulsar. We also report our timing results for this pulsar in this paper.

## 2. Observations

LAT is the main instrument on-board the *Fermi* Gamma-ray Space Telescope. It is a  $\gamma$ -ray imaging instrument which carries out all-sky survey in the energy range from 20 MeV to 300 GeV (Atwood et al. 2009). In our analysis we selected LAT events inside a  $20^\circ \times 20^\circ$  region centered at the position of 2FGL J1906.5+0720 during nearly five-year time period from 2008-08-04 15:43:36 to 2013-07-23 20:53:17 (UTC) from the *Fermi* Pass 7 database. Following recommendations of the LAT team, events included were required to have event zenith angles fewer than 100 deg, preventing contamination from the Earth’s limb, and to be during good time intervals when the quality of the data was not affected by the spacecraft events.

## 3. Analysis and Results

### 3.1. Timing Analysis of PSR J1907+0602

After the *Fermi* discovery of PSR J1907+0602 (Abdo et al. 2009), its timing solution was updated by Abdo et al. (2010) and Ray et al. (2011) using the LAT data during MJD 54647–55074 and MJD 54682–55211, respectively. In 2013 *Fermi*/LAT team released the second *Fermi* catalog of  $\gamma$ -ray pulsars (Abdo et al. 2013), in which the timing solution for PSR J1907+0602 was updated again using the data during MJD 54691–55817. A glitch at MJD 55422 was detected with  $\Delta\nu/\nu$  of  $\sim 4.6 \times 10^{-6}$  and  $\Delta\dot{\nu}/\dot{\nu}$  of  $\sim 1 \times 10^{-2}$ .

In order to better study 2FGL J1906.5+0720 by being able to remove photons from the nearby pulsar, we performed phase-connected timing analysis to the LAT data of J1907+0602 during the nearly five year time period of MJD 54683–56497. We selected LAT events within  $0.7^\circ$  centered at the pulsar’s position given in the catalog in the energy range from 50 MeV to 300 GeV, which was suggested by Ray et al. (2011). Pulse phases for photons before MJD 55800 were assigned according to the known ephemeris using the *Fermi* plugin of TEMPO2 (Edwards et al. 2006; Hobbs et al. 2006). We extracted an ‘empirical Fourier’ template profile, with which we generated the time-of-arrivals (TOAs) of 128 evenly divided observations of the time period. Both the template and TOAs were obtained using the maximum likelihood method described in Ray et al. (2011). We then iteratively fitted the TOAs to the timing model using TEMPO2. From the pre-fit residuals (top panel of Figure 2), we found that the timing model given in the second *Fermi* catalog of  $\gamma$ -ray pulsars could not fully describe the TOAs after MJD  $\sim 55800$ , suggesting a possible glitch besides the known one detected at MJD 55422. We determined the epoch of the possible glitch by requiring continuous pulse phase over the glitch (Yu et al. 2013). A small glitch at MJD  $\sim 55866$  with  $\Delta\nu/\nu$  of  $\sim 1.5 \times 10^{-9}$  and  $\Delta\dot{\nu}/\dot{\nu}$  of

$\sim -3 \times 10^{-4}$  was obtained. Timing results for the pulsar including the locations of the two glitches are shown in the bottom panel of Figure 2, and the updated ephemeris is given in Table 2. The folded pulse profile, test statistic (TS) of H test, and two-dimensional phaseogram of this pulsar are plotted in Figure 3.

We defined phase 0.1–0.7 as the onpulse phase interval and phase 0.7–1.1 as the offpulse phase interval (Figure 3), using the definition given in Abdo et al. (2013).

### 3.2. Maximum Likelihood Analysis

#### 3.2.1. Full data

We selected LAT events in an energy range from 100 MeV to 300 GeV for the likelihood analysis, and included all sources within 15 degrees centered at the position of 2FGL J1906.5+0720 in the *Fermi* 2-year catalog to make the source model. The spectral function forms of the sources are given in the catalog. The spectral normalization parameters for the sources within 4 degrees from 2FGL J1906.5+0720 were left free, and all the other parameters were fixed to their catalog values. In addition we included the spectrum model `gal_2yearp7v6_v0.fits` and the spectrum file `iso_p7v6source.txt` in the source model to consider the Galactic and the extragalactic diffuse emission, respectively. The parameters ‘Value’ of the Galactic diffuse emission model and ‘Normalization’ of the extragalactic diffuse emission model were let free.

In the *Fermi* 2-year catalog, the  $\gamma$ -ray emission from 2FGL J1906.5+0720 is modeled by a log-parabolic law expressed by  $dN/dE = N_0(E/E_b)^{-(\alpha+\beta \ln(E/E_b))}$  (Nolan et al. 2012). We fixed the break energy to the catalog value of  $\sim 1$  GeV, and let the index  $\alpha$  and  $\beta$  free. We also tested two other models for the source: an exponentially cut-off power law expressed by  $dN/dE = N_0 E^{-\Gamma} \exp[-(E/E_{cut})]$ , where  $\Gamma$  is the spectral index and  $E_{cut}$  is the cut-off energy, and a simple power law expressed by  $dN/dE = N_0 E^{-\Gamma}$ . We performed standard binned likelihood analysis with the LAT science tool software package `v9r31p1`. The obtained spectral results and Test Statistic (TS) values are given in Table 3, and the TS map of a  $5^\circ \times 5^\circ$  region around 2FGL J1906.5+0720 is displayed in the left panel of Figure 1. PSR J1907+0602 is kept in the figure to show the proximity of the two sources.

From the analysis, we found that the log-parabolic law and exponentially cut-off power law better fit the LAT data of 2FGL J1906.5+0720 than the simple power law, indicating a significant cutoff in the  $\gamma$ -ray spectrum of 2FGL J1906.5+0720 at the low energy of  $\sim 1$  GeV (Table 3). The significance of the break (approximately described by  $\sqrt{TS_{break}}\sigma = \sqrt{TS_{LP} - TS_{PL}}\sigma$ ) of the log-parabolic law is  $\sim 16\sigma$ , and the significance of the cutoff (approximately described by  $\sqrt{TS_{cutoff}}\sigma = \sqrt{TS_{PL+cutoff} - TS_{PL}}\sigma$ ) of the exponentially cut-off power law is  $\sim 14\sigma$ .

#### 3.2.2. Offpulse phase intervals of PSR J1907+0602

We repeated binned likelihood analysis as described above by including LAT events only during the offpulse phase intervals of PSR J1907+0602. The phase intervals are defined in Section 3.1. Since the emission from the pulsar was removed, we excluded this source from the source model. The likelihood fitting results for the different  $\gamma$ -ray spectral models for 2FGL J1906.5+0720 are

given Table 3, and the TS map of a  $5^\circ \times 5^\circ$  region around 2FGL J1906.5+0720 is plotted in the right panel of Figure 1. The TS values are significantly increased comparing to those when the full data were used, having doubled the detection significance of 2FGL J1906.5+0720. In addition, a low-energy break or cutoff at  $\sim 1$  GeV in the source’s emission is similarly favored as that in the analysis of the full data.

### 3.3. Spectral Analysis

To obtain a spectrum for 2FGL J1906.5+0720, we evenly divided 20 energy ranges in logarithm from 100 MeV to 300 GeV, and used a simple power law to model the emission in each divided energy range. This method is less model-dependent and provides a good description for the  $\gamma$ -ray emission of a source. The spectra from both the full data and the offpulse phase interval data were obtained, which are displayed in Figure 4.

We plotted the obtained exponentially cut-off power-law fits and log-parabolic law fits from the above likelihood analysis in Figure 4. As can be seen, the first model does not provide a good fit to the LAT spectrum. At energies of greater than several GeV, the fits deviate from the spectrum both for the full data and the offpulse phase interval data of PSR J1907+0602. The log-parabolic law better describes the spectra, which is also indicated by the larger TS values obtained with it (Table 3), although a small degree of deviations from the spectra can still be seen. These may suggest an additional spectral component at the high energy range.

We fit the spectral data points below 2 GeV with exponentially cut-off power laws and obtained  $\Gamma$  of  $1.4 \pm 0.2$  and  $E_{cutoff}$  of  $1.0 \pm 0.2$  GeV from the full data, and  $\Gamma$  of  $1.6 \pm 0.1$  and  $E_{cutoff}$  of  $0.7 \pm 0.1$  GeV from the offpulse phase interval data. The cutoff energy values are within the range of young  $\gamma$ -ray pulsars ( $0.4 < E_{cutoff} < 5.9$ ; see Table 9 in Abdo et al. 2013) but lower than that of millisecond  $\gamma$ -ray pulsars ( $1.1 < E_{cutoff} < 5.4$ ; see Table 9 in Abdo et al. 2013). The fitting again shows that an additional spectral component is needed.

### 3.4. Spatial Distribution Analysis

In the residual TS maps both from the full data and the offpulse phase interval data after removing all sources (Figure 1), two  $\gamma$ -ray emission excesses exist. They are located at R.A.= $285^\circ 326$  and Decl.=  $5^\circ 855$  (equinox J2000.0), with  $1\sigma$  error circle of  $0^\circ 07$ , and R.A.= $285^\circ 293$  and Decl.=  $7^\circ 030$  (equinox J2000.0), with  $1\sigma$  error circle of  $0^\circ 1$  (marked by circles in Figure 1), which were obtained from running ‘gtfindsrc’ in LAT science tools software package. In addition, there is also a tail-like structure in the southeast direction of 2FGL J1906.5+0720, which can be clearly seen in the TS map during offpulse intervals. In order to determine whether this tail structure is associated with 2FGL J1906.5+0720 or caused by the two nearby sources, we further performed maximum likelihood analysis by including the two sources in the source model. The emission of the two putative sources were modeled by a simple power law. We found that the tail structure was completely removed (see the left panel of Figure 5), indicating that it is likely caused by the two nearby sources.

A  $\gamma$ -ray spectrum of 2FGL J1906.5+0720 was obtained again for the offpulse phase interval

data, with the two nearby sources considered. The three spectral models given in Section 3.2 were used. The results are given in Table 3. The spectral parameter values are similar to those obtained above. We also fit the obtained spectral data points below 2 GeV with an exponentially cut-off power law (cf. Section 3.3). Nearly the same results were obtained (Table 3).

These analyses confirm the existence of a high-energy component in the emission of 2FGL J1906.5+0720, which is likely not to be caused by contamination from the nearby sources. By constructing TS maps with photons greater than 2 or 5 GeV, we searched for extended emission (e.g., a pulsar wind nebula) at the position of 2FGL J1906.5+0720. However, the source profile was always consistent with being a point source. There was no indication for the existence of an additional source responsible for the high-energy component.

### 3.5. Timing analysis of 2FGL J1906.5+0720

Timing analysis was performed to the LAT data of 2FGL J1906.5+0720 to search for  $\gamma$ -ray pulsation signals. We included events in the energy range from 50 MeV to 300 GeV within 1 degree centered at the position of 2FGL J1906.5+0720 during a 300-day period from 2012-09-26 20:53:17 to 2013-07-23 20:53:17 (UTC), and applied a time-differencing blind search technique described in Atwood et al. (2006). The range of frequency derivative  $\dot{\nu}$  over frequency  $\nu$  we considered was  $|\dot{\nu}/\nu| = 0-1.3 \times 10^{-11} \text{ s}^{-1}$ , which is characteristic of pulsars such as the Crab pulsar. A step of  $2.332 \times 10^{-15} \text{ s}^{-1}$  was used in the search. The frequency range we considered was from 0.5 Hz to 32 Hz with a Fourier resolution of  $1.90735 \times 10^{-6} \text{ Hz}$ . We did not include the parameter ranges characteristic of millisecond pulsars. The source 2FGL J1906.5+0720 is located in the Galactic plane and would be possibly a young pulsar such as PSR J1907+0602. No significant  $\gamma$ -ray pulsations from 2FGL J1906.5+0720 were detected. We also applied the blind search to *Fermi*/LAT data of 2FGL J1906.5+0720 only during the offpulse phase intervals of PSR J1907+0602. No  $\gamma$ -ray pulsations except the spin frequency signal of PSR J1907+0602 were found.

In addition, we also searched for any long-period modulations from the source, the detection of which would be indicative of a binary system (see discussion in Section 4). We constructed power spectra during offpulse phase intervals of PSR J1907+0602 in the three energy bands of 0.2–1 GeV, 1–300 GeV, and 5–300 GeV. Light curves of nearly five-year length in the three energy bands were extracted from performing *Fermi*/LAT aperture photometry analysis. The aperture radius was 1 degree, and the time resolution of the light curves was 1000 seconds. The exposures were calculated assuming power law spectra with photon indices obtained by maximum likelihood analysis (Table 3), which were used to determine the flux in each time bin. No long-period modulations in the energy bands were found.

## 4. Discussion

By carrying out phase-connected timing analysis of the *Fermi*  $\gamma$ -ray data of PSR J1907+0602, we found a likely small glitch around MJD 55866. This glitch has a small frequency increment that

results in large uncertainties on the epoch determination. The deviations of the prefit residuals after MJD  $\sim 55800$  is not sharp (see Figure 2). These features make it difficult to distinguish the glitch from timing noise. However, considering no timing noise was reported for this pulsar before (Abdo et al. 2010; Ray et al. 2011; Abdo et al. 2013), a small glitch at around MJD 55866 is the likely case. The glitch has the smallest  $\Delta\nu/\nu$  value among those detected by *Fermi* (the smallest  $\Delta\nu/\nu$  reported in the second *Fermi* catalog of  $\gamma$ -ray pulsars is  $2.7 \times 10^{-8}$ ; Abdo et al. 2013).

We performed different analyses of the *Fermi*/LAT data for the unassociated source 2FGL J1906.5+0720. Through likelihood analysis with different spectral models, we confirmed that a curved spectrum with a low-energy break or cutoff at  $\sim 1$  GeV is clearly preferred to a simple power law. The significances of the curvature ( $\sim \sqrt{TS}\sigma$ ) are approximately 14–16  $\sigma$  and 16–18  $\sigma$  for the full data and the offpulse phase interval data, respectively. This feature is characteristic of  $\gamma$ -ray pulsars detected by *Fermi*. On the basis of the *Fermi* second pulsar catalog, young  $\gamma$ -ray pulsars have  $0.6 < \Gamma < 2$  and  $0.4 \text{ GeV} < E_{\text{cutoff}} < 5.9 \text{ GeV}$ , and millisecond  $\gamma$ -ray pulsars have  $0.4 < \Gamma < 2$  and  $1.1 \text{ GeV} < E_{\text{cutoff}} < 5.4 \text{ GeV}$  (Abdo et al. 2013). If 2FGL J1906.5+0720 is a pulsar, its Galactic location and spectral feature suggest that it is probably a young pulsar (see, e.g., Abdo et al. 2013).

We note that a second spectral component, in addition to the exponentially cutoff power law, has been found in the emission from the crab pulsar and the black-widow pulsar PSR B1957+20. The first and the latter have a  $\sim 100$  GeV (Aharonian et al. 2012) and  $\sim 3$  GeV (Wu et al. 2012) component, respectively. The component is suggested to be due to a cold pulsar wind from them, high-energy particles of which do not interact with surrounding material but inverse-Compton scatter low-energy photons from the magnetosphere (for the Crab pulsar, Aharonian et al. (2012)) or from the companion (for PSR B1957+20, Wu et al. (2012)) to  $\gamma$ -ray photons. The additional component has also been detected in the  $\gamma$ -ray binary systems PSR B1259–63 (Khargulyan et al. 2012), LS I +61°303 and LS 5039 (Hadasch et al. 2012). A log-parabolic law, which better fits the spectra of 2FGL J1906.5+0720, is usually used to model the spectra of  $\gamma$ -ray binaries (Nolan et al. 2012). The origin for the emission excesses is suggested to be a cold wind too for PSR B1259–63 (a 47.7 ms pulsar with a high-mass Be star companion; Aharonian et al. 2009; Abdo et al. 2011), but not clear for LS I +61°303 and LS 5039. Considering the non-detection of any long-period modulations and the low variability of 2FGL J1906.5+0720, a  $\gamma$ -ray binary is not likely the case for the source.

We have not been able to find any pulsed emission signals from the *Fermi* data of 2FGL J1906.5+0720, which is required to verify the source’s pulsar nature. However, we note that the LAT blind search sensitivity depends on many parameters, such as the accurate position of the source, the source region used for pulsation search, contamination from background diffuse emission and from nearby sources (given that our target is located at the Galactic plane with several identifiable sources nearby). Based on the emission properties obtained from our different data analyses for 2FGL J1906.5+0720, this *Fermi* unassociated source is likely a pulsar. In order to confirm its pulsar nature, radio search for pulse signals is needed.

This research was supported by Shanghai Natural Science Foundation for Youth (13ZR1464400) and National Natural Science Foundation of China (11373055). ZW is a Research Fellow of the One-Hundred-Talents project of Chinese Academy of Sciences.



**Table 1.** The first 10 candidate pulsars ranked by Signif\_Curve

Source	Signif_Curve ( $\sigma$ )	$Gb$ ( $^\circ$ )	Variability_Index	Signif_Avg ( $\sigma$ )
2FGL J1704.9–4618	9.96616	–3.11145	21.3407	9.31067
2FGL J1906.5+0720	9.84956	–0.00205713	30.8941	23.9589
2FGL J1819.3–1523	9.24969	–0.0720518	30.0403	19.2914
2FGL J1847.2–0236	8.52713	–0.256826	31.2966	13.8065
2FGL J1856.2+0450c	8.38407	1.13861	18.7873	12.2946
2FGL J1619.0–4650	8.30750	2.45675	22.2354	10.5751
2FGL J2033.6+3927	8.27851	–0.381993	33.7517	13.0404
2FGL J1045.0–5941	8.27539	–0.639366	21.4889	36.0695
2FGL J0858.3–4333	8.12207	1.42752	16.4655	14.1381
2FGL J1739.6–2726	8.07930	1.90624	27.6240	15.2077

**Table 2.**  $\gamma$ -ray ephemeris for PSR J1907+0602.

Parameter	Value*
R.A., $\alpha$ (J2000.0)	19:07:54.74 $\pm$ 0 <sup>s</sup> .004
Decl., $\delta$ (J2000.0)	06:02:16.65 $\pm$ 0 <sup>s</sup> .12
Pulse frequency, $\nu$ (s <sup>-1</sup> )	9.37766094207(5)
Frequency first derivative, $\dot{\nu}$ (s <sup>-2</sup> )	$-7.627459(1) \times 10^{-12}$
Frequency second derivative, $\ddot{\nu}$ (s <sup>-3</sup> )	$1.9220(8) \times 10^{-22}$
Epoch of frequency (MJD)	55422.275976
Dispersion measure (cm <sup>-3</sup> pc)	82.1
1st glitch epoch (MJD)	55422.186914
1st glitch permanent frequency increment (s <sup>-1</sup> )	$4.3533(4) \times 10^{-5}$
1st glitch frequency deriv increment (s <sup>-2</sup> )	$-7.90(2) \times 10^{-14}$
1st glitch frequency increment (s <sup>-1</sup> )	$2.6(1) \times 10^{-7}$
1st glitch decay time (Days)	36(2)
2nd glitch epoch (MJD)	$\sim$ 55866
2nd glitch permanent frequency increment (s <sup>-1</sup> )	$1.4(3) \times 10^{-8}$
2nd glitch frequency deriv increment (s <sup>-2</sup> )	$1.98(7) \times 10^{-15}$
$E_{min}$	50 MeV
Valid range (MJD)	54683–56497

\* Parameters with no uncertainty reported are fixed to the values given in the second *Fermi* catalog of  $\gamma$ -ray pulsar (Abdo et al. 2013).

**Table 3.** Maximum binned likelihood results for 2FGL J1906.5+0720

Spectral model	Parameters	Full data	Offpulse phase interval data	Offpulse phase interval data (‘tail’ removed)
PowerLaw	$\Gamma$	$2.31 \pm 0.02$	$2.42 \pm 0.02$	$2.31 \pm 0.02$
	$G_\gamma$ ( $10^{-11}$ erg cm $^{-2}$ s $^{-1}$ )	$15 \pm 0.5$	$13 \pm 0.4$	$11 \pm 0.4$
	$TS_{PL}$	1101	2437	1595
LogParabola	$\alpha$	$2.52 \pm 0.05$	$2.82 \pm 0.05$	$2.73 \pm 0.07$
	$\beta$	$0.35 \pm 0.03$	$0.37 \pm 0.03$	$0.51 \pm 0.04$
	$E_b^*$ (GeV)	1	1	1
	$G_\gamma$ ( $10^{-11}$ erg cm $^{-2}$ s $^{-1}$ )	$13 \pm 0.5$	$12 \pm 0.4$	$9 \pm 0.3$
	$TS_{LP}$	1388	2795	1966
PLSuperExpCutoff	$\Gamma$	$1.7 \pm 0.2$	$1.7 \pm 0.1$	$1.2 \pm 0.1$
	$E_{cut}$ (GeV)	$1.7 \pm 0.8$	$1.2 \pm 0.2$	$0.8 \pm 0.1$
	$G_\gamma$ ( $10^{-11}$ erg cm $^{-2}$ s $^{-1}$ )	$13 \pm 5$	$12 \pm 2$	$9 \pm 1$
	$TS_{PL+cutoff}$	1297	2694	1853
PLSuperExpCutoff obtained by fitting	$\Gamma$	$1.4 \pm 0.3$	$1.4 \pm 0.1$	$1.4 \pm 0.2$
	$E_{cut}$ (GeV)	$1.0 \pm 0.3$	$0.5 \pm 0.1$	$0.6 \pm 0.1$

\* The break energies are fixed at 1 GeV.

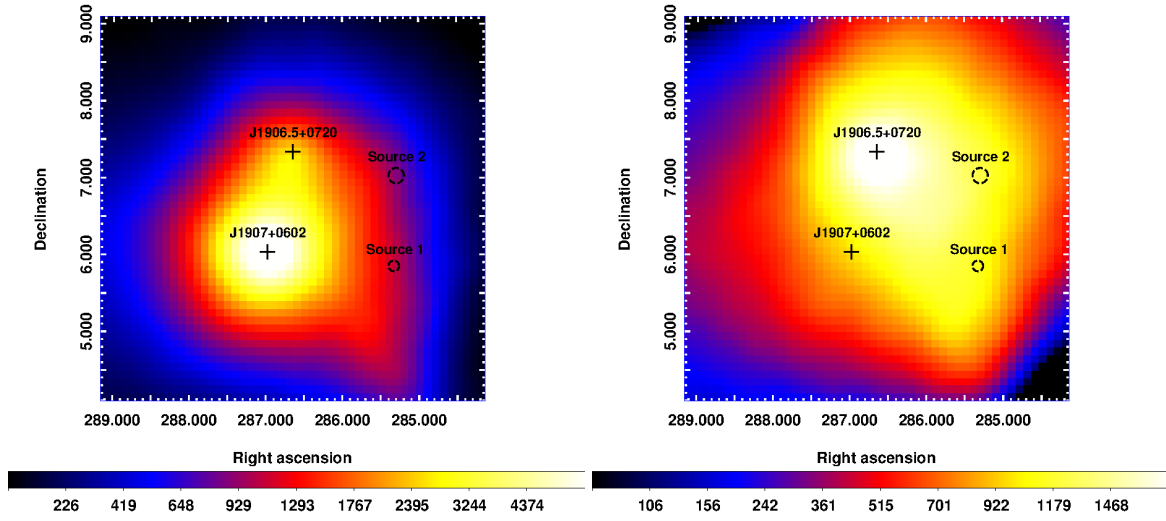


**Fig. 1.** TS maps (0.1–300 GeV) of  $5^\circ \times 5^\circ$  regions centered at R.A.=  $286.647^\circ$ , Decl.=  $6.6^\circ$  (equinox J2000.0) extracted from the full data (*left* panel) and offpulse phase interval data (*right* panel) of PSR J1907+0602. The image scales of the maps are  $0.1 \text{ pixel}^{-1}$ . Two putative nearby sources are marked by circles.

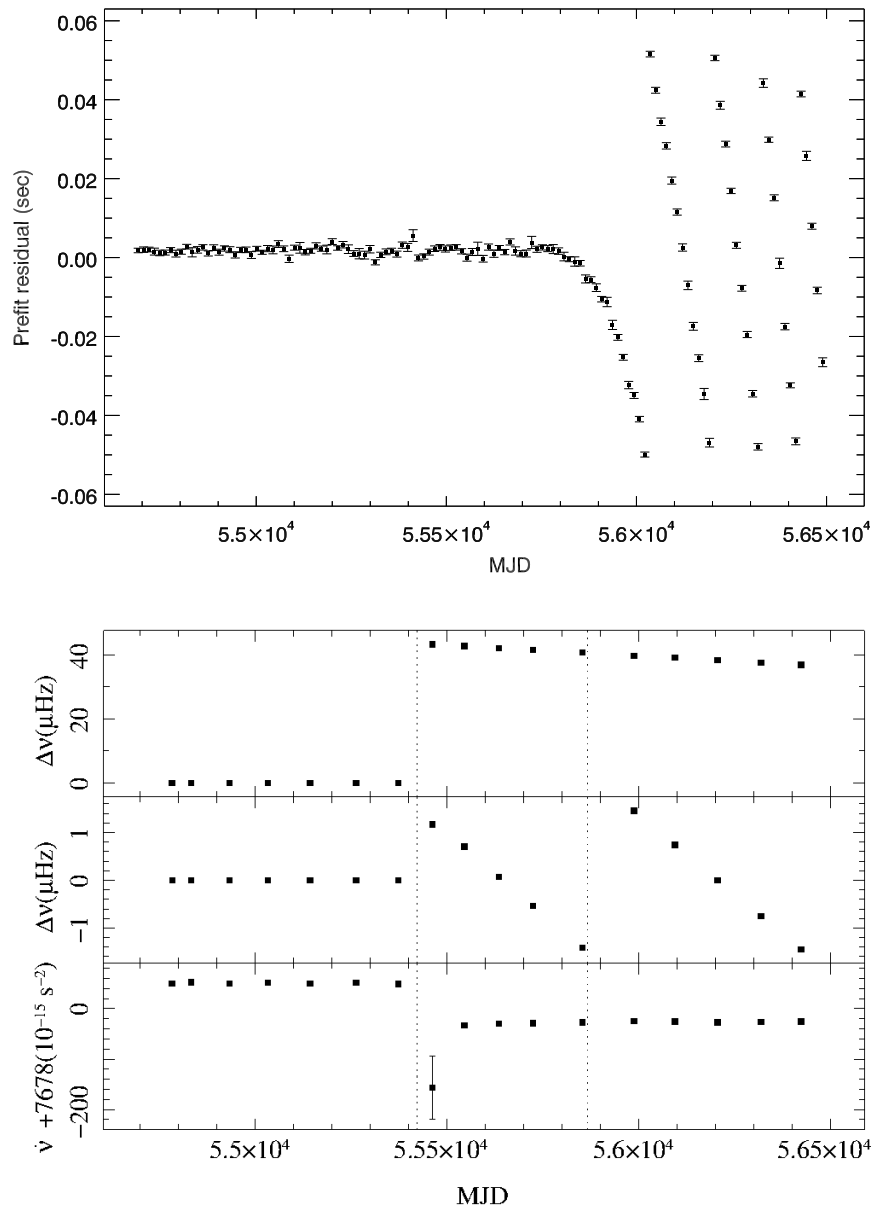


**Fig. 2.** *Top panel:* Pre-fit timing residuals of PSR J1907+0602. *Bottom panel:* Post-fit timing results for PSR J1907+0602. The positions of two glitches are marked by dotted lines.

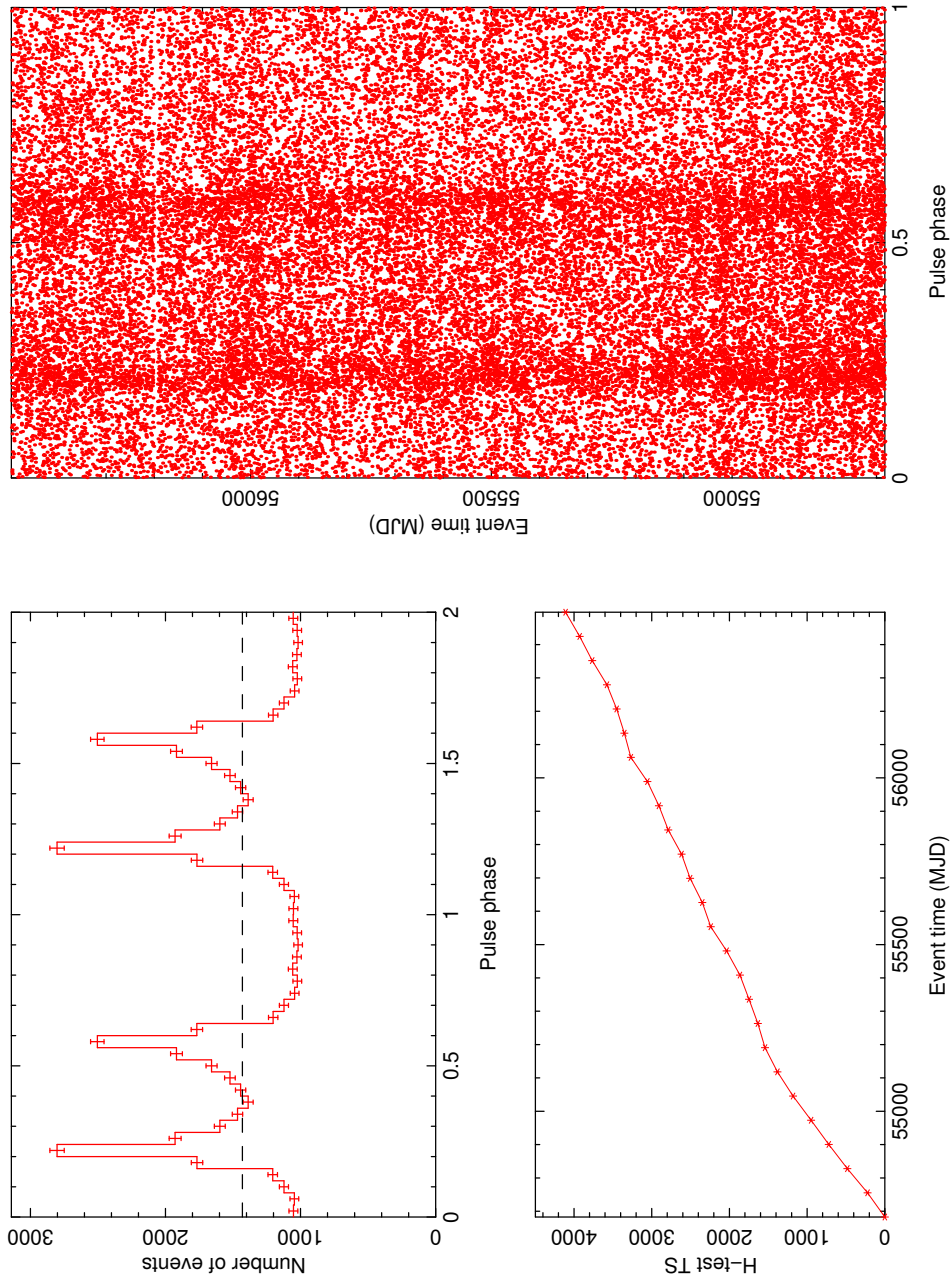


**Fig. 3.** Folded pulse profile, Test Statistic of H test, and two-dimensional phaseogram obtained for PSR J1907+0602.

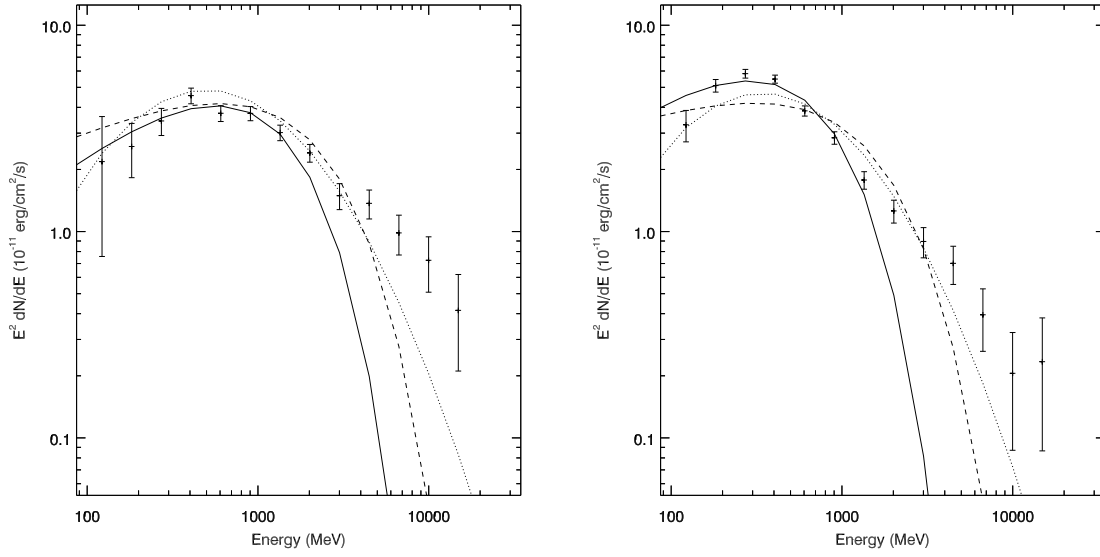


**Fig. 4.**  $\gamma$ -ray spectra of 2FGL J1906.5+0720 extracted from the full data (*left* panel) and offpulse phase interval data (*right* panel). The exponentially cut-off power laws and the log-parabolic laws obtained from maximum likelihood analysis (see Table 3) are displayed as dashed and dotted curves. The solid curves are the exponentially cut-off power laws obtained by fitting the data points below 2 GeV.

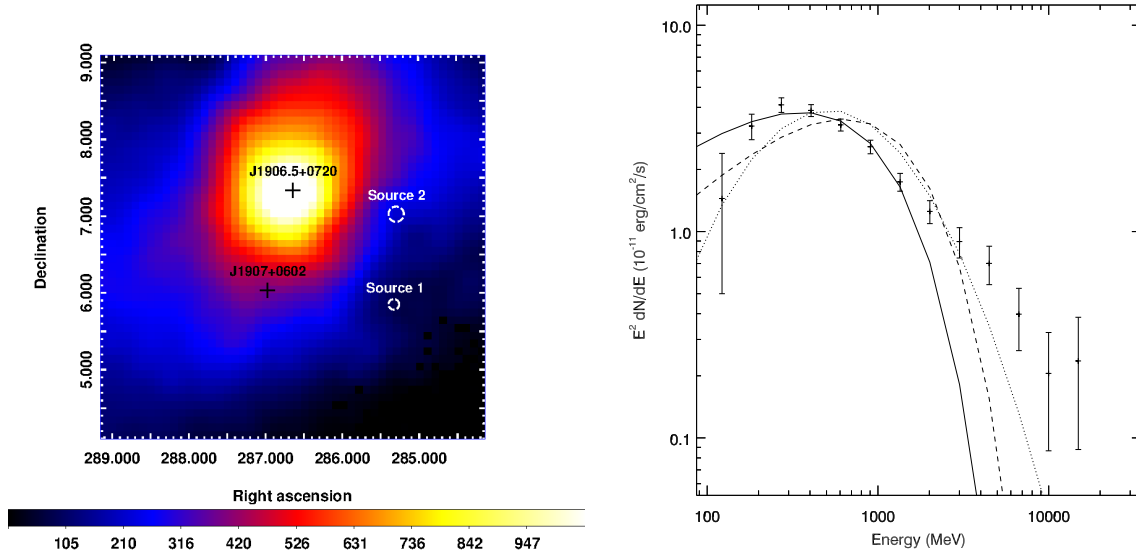


**Fig. 5.** *Left panel:* TS map (0.1–300 GeV) of  $5^\circ \times 5^\circ$  region centered at R.A.= 286.647°, Decl.= 6.6° (equinox J2000.0) extracted from the offpulse phase interval data of PSR J1907+0602 when the two nearby sources (the positions are marked by circles) were removed. The image scale of the map is  $0.1 \text{ pixel}^{-1}$ . *Right panel:*  $\gamma$ -ray spectrum of 2FGL J1906.5+0720 extracted from the offpulse phase interval data when the two nearby sources were removed. The dashed and dotted curves represent the exponentially cut-off power law and the log-parabolic law, respectively, obtained from maximum likelihood analysis (see Table 3). The solid curve represents the exponentially cut-off power law obtained by fitting the data points below 2 GeV.



## References

- Abdo, A. A., Ackermann, M., Ajello, M., et al. 2009, *Science*, 325, 840  
— . 2010, *ApJ*, 711, 64  
— . 2011, *ApJL*, 736, L11
- Abdo, A. A., Ajello, M., Allafort, A., et al. 2013, *ApJS*, 208, 17
- Ackermann, M., Ajello, M., Baldini, L., et al. 2011, *ApJ*, 726, 35
- Aharonian, F., Akhperjanian, A. G., Anton, G., et al. 2009, *A&A*, 507, 389
- Aharonian, F. A., Bogovalov, S. V., & Khangulyan, D. 2012, *Nature*, 482, 507
- Atwood, W. B., Ziegler, M., Johnson, R. P., & Baughman, B. M. 2006, *ApJL*, 652, L49
- Atwood, W. B., Abdo, A. A., Ackermann, M., et al. 2009, *ApJ*, 697, 1071
- Barr, E. D., Guillemot, L., Champion, D. J., et al. 2013, *MNRAS*, 429, 1633
- Cheng, K. S., Ho, C., & Ruderman, M. 1986, *ApJ*, 300, 500
- Cheng, K. S., Taam, R. E., & Wang, W. 2004, *ApJ*, 617, 480
- Edwards, R. T., Hobbs, G. B., & Manchester, R. N. 2006, *MNRAS*, 372, 1549
- Hadasch, D., Torres, D. F., Tanaka, T., et al. 2012, *ApJ*, 749, 54
- Hobbs, G. B., Edwards, R. T., & Manchester, R. N. 2006, *MNRAS*, 369, 655
- Khangulyan, D., Aharonian, F. A., Bogovalov, S. V., & Ribó, M. 2012, *ApJL*, 752, L17
- Komissarov, S. S., & Lyubarsky, Y. E. 2004, *MNRAS*, 349, 779
- Lee, K. J., Guillemot, L., Yue, Y. L., Kramer, M., & Champion, D. J. 2012, *MNRAS*, 424, 2832
- Malyshev, D., Zdziarski, A. A., & Chernyakova, M. 2013, *MNRAS*, 434, 2380
- Nolan, P. L., Abdo, A. A., Ackermann, M., et al. 2012, *ApJS*, 199, 31
- Pletsch, H. J., Guillemot, L., Fehrmann, H., et al. 2012a, *Science*, 338, 1314
- Pletsch, H. J., Guillemot, L., Allen, B., et al. 2012b, *ApJ*, 744, 105
- Ransom, S. M., Ray, P. S., Camilo, F., et al. 2011, *ApJL*, 727, L16
- Ray, P. S., Kerr, M., Parent, D., et al. 2011, *ApJS*, 194, 17
- Saz Parkinson, P. M., Dormody, M., Ziegler, M., et al. 2010, *ApJ*, 725, 571
- Takata, J., Shibata, S., Hirotani, K., & Chang, H.-K. 2006, *MNRAS*, 366, 1310
- Wu, E. M. H., Takata, J., Cheng, K. S., et al. 2012, *ApJ*, 761, 181
- Yu, M., Manchester, R. N., Hobbs, G., et al. 2013, *MNRAS*, 429, 688